25th ABCM International Congress of Mechanical Engineering
October 20-25, 2019, Uberlândia, MG, Brazil

COBEM2019-0814
A MODEL-BASED CRACK IDENTIFICATION APPROACH

Leandro de Souza Leão
Iago Alves Pereira
Aldemir Aparecido Cavalini Junior
Valder Steffen Junior
LMEst – Structural Mechanics Laboratory, Federal University of Uberlândia, School of Mechanical Engineering, Av. João Naves de Ávila, 2121, Uberlândia, MG, 38408-196, Brazil
leao@ufu.br
iagoufu@gmail.com
aacjunior@ufu.br
vsteffen@ufu.br

Abstract. *In the present contribution, a model-based crack detection approach devoted to rotating machines is investigated. The method can identify the location and depth of transverse cracks in rotating machines by analyzing their lateral vibrations. The rotor model is obtained by using the finite element method, considering the Timoshenko beam theory. The crack is applied considering the Mayes' model. The identification process is based on the solution of an inverse problem, in which the operational vibration responses of the rotor are correlated with the associated numerical data. An optimization algorithm is formulated to identify cracks with different depths and locations along with the rotor model. The vibration responses are continually compared. When the optimization code fits the numerical and the operational vibration responses of the rotor, the location and depth of the crack are identified. The so-called Differential Evolution technique is used to solve the mentioned inverse problem. This method is purely a mathematical approach, performing vector combinations that define new search directions over the objective function. The rotating machine used in this work is composed by a flexible horizontal shaft, containing two rigid discs, and is supported by self-alignment ball bearings located at both ends of the shaft. The results demonstrate the possibility of identifying the location and depth of transverse cracks along with the rotor.*

Keywords: *rotordynamics, model-based approach, crack identification, differential evolution.*

1. INTRODUCTION

An accident motivated the development of health monitoring techniques devoted to crack detection in shafts of rotating machines that occurred in a General Electric turbine in the early 1970s. A considerable academic effort on crack detection techniques was verified in the 1980s, resulting in high economic impact in various industries (Dimarogonas *et al*., 2013). Researches on structural health monitoring (SHM) techniques for early crack detection has been growing since then. According to Cavalini Jr *et al*. (2015), there are several SHM techniques proposed in the literature for crack detection in rotating machines. Visual examination, radiographic tests, ultrasonic tests, and dye penetrant inspection, are some examples of nondestructive techniques widely used for crack detection. These methods have proved to be costly since satisfactory results rely on detailed and periodic inspections (Saavedra and Cuitiño, 2001). The full stop of the machinery is required for the examinations, implying in production losses which are proportional to the time spent on verification. Therefore, techniques based on vibration measurements are recognized as promising SHM tools (Structural Health Monitoring) and significant research effort has been directed in the recent years to crack detection, location, and severity estimation by using vibration signals (Doebling *et al*., 1998; Darpe *et al*., 2004; Cavalini Jr *et al*., 2015).

The online inspections based on vibration measurements allow continuous verification of the machine condition. These SHM techniques help to increase the equipment lifetime and the reliability in operation throughout the aging of the system. The SHM techniques based on the vibration signals are sensitive to mass, damping, or stiffness changes on the structure, indicating the presence of a crack (Carden and Fanning, 2004). According to Zhao (2013), the so-called model-based approach devoted to fault detection in mechanical systems was firstly proposed by Isermann (1995). The developed technique was applied in various mechanical systems, such as electric motors, actuators, pumps, machine tools, etc. Bachschmid *et al*. (2000) presented the possibility of identifying the crack configuration in a rotating machine by using a model-based technique allied to the 1X, 2X, and 3X harmonic components of the vibration responses. Markert *et al*. (2001) proposed a model-based approach in which the crack was identified relating the fault parameters

with fictitious equivalent forces. Sawicki *et al*. (2011) have experimentally detected a crack by applying a specified harmonic force on the rotor using a single magnetic bearing. The rotor used in this work was composed of a shaft supported by two active magnetic bearings and one disc located at the shaft middle span. The presence of the damage led to spectral responses with additional peaks at frequencies that are combinations of the rotor speed, its critical speed, and the frequency of the diagnostic force. The authors concluded that this method could result in a fast and convenient approach to damage detection.

In this context, the present work aims at presenting a model-based approach able to identify the depth and location of transversal cracks in shafts of rotating machines. A representative dynamic model of the system (i.e., finite element model – FE model) and continuously measured vibration signals are required to perform the proposed online fault monitoring. The crack identification process involves the solution of a typical inverse problem. Once the physical model of the rotating machine is known, the acquired experimental signals and the theoretical responses are put together using a given objective function to be minimized and evaluate the health condition of the rotor. If the procedure converges to a minimum value of the objective function, the crack is identified. If this is not the case, the optimization procedure will propose a new crack configuration (i.e., depth and location). The optimization process continues until convergence is achieved. The heuristic optimization technique known as Differential Evolution (Storn and Price, 1995) is used in this work to identify the severity of the crack.

2. ROTOR TEST RIG

Figure 1a shows the rotor test rig used in the numerical simulations presented in this work, which was mathematically represented by a model with 33 finite elements (Timoshenko's beam elements with 4 degrees of freedom per node; Fig. 1b). It is composed by a flexible steel shaft with 860 mm length and 17 mm of diameter (E = 205 GPa, ρ = 7850 kg/m^3, υ = 0.29), two rigid discs D_1 (node #13; 2.637 kg) and D_2 (node #23; 2.649 kg), both of steel and with 150 mm of diameter and 20 mm of thickness (ρ = 7850 kg/m^3), and two roller bearings (B_1 and B_2, located at the nodes #4 and #31, respectively). Displacement sensors are orthogonally mounted on the nodes #8 (S_{8X} and S_{8Z}) and #28 (S_{28X} and S_{28Z}) to collect the shaft vibration. An electric DC motor drives the system. Also, a crack located at the element #20 and different depths will be considered to be identified by the SHM technique (see Fig. 1b).

Equation 1 presents the equation of motion that governs the dynamic behavior of the cracked flexible rotor supported by roller bearings (Lalanne and Ferraris, 1998).

$$\mathbf{M}\ddot{\mathbf{q}} + \left[\mathbf{D} + \Omega\mathbf{D}_g\right]\dot{\mathbf{q}} + \left[\mathbf{K} + \dot{\Omega}\mathbf{K}_{st}\right]\mathbf{q} = \mathbf{W} + \mathbf{F}_u + \mathbf{F}_m + \Delta\mathbf{K}\mathbf{q} \tag{1}$$

where $\mathbf{M}$ is the mass matrix, $\mathbf{D}$ is the damping matrix, $\mathbf{D}_g$ is the gyroscopic matrix, $\mathbf{K}$ is the stiffness matrix, and $\mathbf{K}_{st}$ is the stiffness matrix resulting from the transient motion. All these matrices are related to the rotating parts of the system, such as couplings, discs, and shaft. $\mathbf{W}$ stands for the weight of the rotating parts, $\mathbf{F}_u$ represents the unbalance forces, $\mathbf{F}_m$ is the vector of the shaft supporting forces produced by the roller bearings, and $\mathbf{q}$ is the generalized displacement vector. $\mathbf{\Delta K}$ represents the maximum stiffness variation due to the crack presence, which is modeled according to Mayes' model (Cavalini-Jr. et al., 2016).

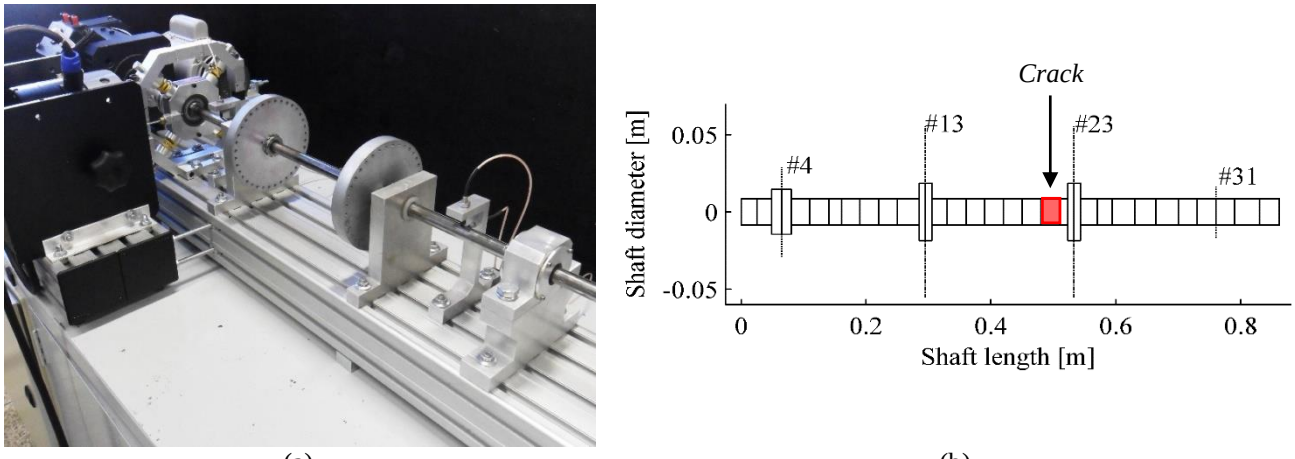

(a) (b)

Figure 1. Rotor test rig used in the numerical simulations of the SHM technique: a) Test rig; b) FE model.

A model updating procedure was used to obtain a representative healthy FE model (Fig. 1b; for $\Delta\mathbf{K}$ = 0 in Eq. (1)). In this sense, a heuristic optimization technique (DE) was used to determine the unknown parameters of the FE model. Thus, the stiffness and damping coefficients of the bearings, the proportional damping added to $\mathbf{D}$ (coefficients γ and β;

D = γ **M** + β **K**), and the angular stiffness k_{ROT} due to the coupling between the electric motor and the shaft (added around the orthogonal directions *X* and *Z* of the node #1) were determined.

The entire frequency domain model updating process (i.e., comparison between simulated and experimental frequency response functions, FRF) was performed 10 times, considering 100 individuals in the initial population of the optimizer. However, in this case, only the regions close to the peaks associated with the natural frequencies were considered. Table 1 summarizes the parameters determined at the end of the minimization process associated with the smaller fitness value (i.e., the value of the objective function). Figure 2 compares simulated and experimental FRF, and related phase diagram, considering the parameters shown in Tab. 1. More details about the model update procedure adopted in this work can be found in Cavalini Jr *et al.* (2016), or in Morais *et al.* (2013), which presents a similar approach for model updating.

Table 1. Parameters determined by the model updating procedure.

Parameters	Values	Parameters	Values	Parameters	Values
k_X / B_1	8.551 *x* 10^5	k_X / B_2	5.202 *x* 10^7	γ	2.730
k_Z / B_1	1.198 *x* 10^6	k_Z / B_2	7.023 *x* 10^8	β	4.85 *x* 10^{-6}
d_X / B_1	7.452	d_X / B_2	25.587	k_{ROT}	770.442
d_Z / B_1	33.679	d_Z / B_2	91.033		

*k: stiffness [N/m]; d: damping [Ns/m].

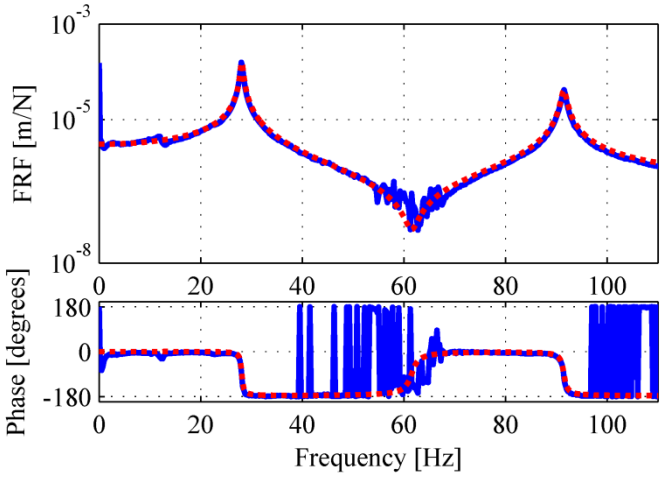

Figure 2. Simulated (- - -) and experimental (——) FRF and associated phases obtained from impact forces on D1 (X direction and S8X).

3. CRACK MODEL

Two models are currently used to represent the breathing behavior with weight dominance, namely the models proposed by R. Gasch (Gasch, 1976) and I.W. Mayes and W.G.R. Davies (Mayes and Davies, 1976). However, these models are not able to correlate the increased flexibility of a shaft element according to the depth of the crack. Thus, in the present contribution, the additional flexibility is calculated by using the linear fracture mechanics theory. This formulation is interesting since it gives the stiffness matrix of the element containing the crack explicitly in terms of its depth. Different formulations able to correlate the flexibility of the shaft element with the crack depth are found in the literature.

The Mayes' model is based on a cosine function that allows a smooth transition between the fully opened and fully closed crack. The stiffness along the η and ξ directions (Fig. 3, where Ω is the rotating speed of the rotor and t is the time) according to the Mayes' model ($k_{\eta Mayes}$ and $k_{\xi Mayes}$, respectively, in the rotating coordinates) are defined by Eq. (2).

$$k_{\xi Mayes}(\theta) = \frac{1}{2}\left(k_o + k_\xi\right) + \frac{1}{2}\left(k_o - k_\xi\right)C_1$$
$$k_{\eta Mayes}(\theta) = \frac{1}{2}\left(k_o + k_\eta\right) + \frac{1}{2}\left(k_o - k_\eta\right)C_1 \quad (2)$$

where $C_1 = cos\ \theta$ ($C_i = cos\ i\theta$; i = 1, 2, 3, …), k_o is the stiffness of the shaft without crack; k_η and k_ξ are the stiffness of the shaft with a crack along with the directions η and ξ, respectively. If C_1 = 1, i.e., for $\theta = 0^0$, $k_{\xi Mayes}$ (0^0) = k_o and

$k_{\eta Mayes}$ (0^0) = k_o. Thus, the crack remains fully closed. However, if C_1 = –1, i.e., for θ = 180^0, $k_{\xi Mayes}$ (180^0) = k_ξ and $k_{\eta Mayes}$ (180^0) = k_η. In this case, the crack remains fully opened (Burbano and Steffen Jr, 2007).

The stiffness of the cracked shaft in rotating coordinates ($\mathbf{k}_{RMayes}$ in a matrix representation according to the Mayes' model) is given by:

$$\mathbf{k}_{RMayes} = \begin{bmatrix} k_{M\xi} + k_{D\xi} C_1 & 0 \\ 0 & k_{M\eta} + k_{D\eta} C_1 \end{bmatrix} \tag{3}$$

where $k_{M\xi} = (k_o + k_\xi) / 2$, $k_{M\eta} = (k_o + k_\eta) / 2$, $k_{D\xi} = (k_o - k_\xi) / 2$, and $k_{D\eta} = (k_o - k_\eta) / 2$.

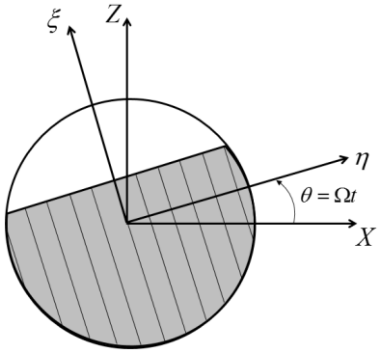

Figure 3. Fixed and rotating coordinates for the cracked shaft.

On the other hand, the stiffness of the cracked shaft in fixed coordinates ($\mathbf{k}_{FMayes}$ in a matrix representation) is determined from a mathematic transformation, as shown in the Eq. (4).

$$\mathbf{k}_{FMayes} = \begin{bmatrix} C_1 & S_1 \\ -S_1 & C_1 \end{bmatrix}^T \mathbf{k}_{RMayes} \begin{bmatrix} C_1 & S_1 \\ -S_1 & C_1 \end{bmatrix} = \begin{bmatrix} k_{FMayes(11)} & k_{FMayes(12)} \\ k_{FMayes(12)} & k_{FMayes(22)} \end{bmatrix} \tag{4}$$

where $S_i = sin\, i\theta$ (i = 1, 2, 3, …). Thus, the terms of $\mathbf{k}_{FMayes}$ are given by:

$$\begin{aligned} k_{FMayes(11)} &= \frac{1}{2}\left(k_{M\xi} - k_{M\eta}\right) + \frac{1}{4}\left(3k_{D\xi} - k_{D\eta}\right)C_1 + \frac{1}{4}\left(k_\xi - k_\eta\right)C_2 - \frac{1}{8}\left(k_\xi - k_\eta\right)C_3 \\ k_{FMayes(22)} &= \frac{1}{2}\left(k_{M\xi} + k_{M\eta}\right) + \frac{1}{4}\left(k_{D\xi} - 3k_{D\eta}\right)C_1 - \frac{1}{4}\left(k_\xi - k_\eta\right)C_2 - \frac{1}{8}\left(k_\xi - k_\eta\right)C_3 \\ k_{FMayes(12)} &= \frac{1}{4}\left(k_{D\xi} - k_{D\eta}\right)S_1 + \frac{1}{2}\left(k_{M\xi} - k_{M\eta}\right)S_2 + \frac{1}{4}\left(k_{D\xi} - k_{D\eta}\right)S_3 \end{aligned} \tag{5}$$

The stiffness matrix of the shaft element with the transverse crack $\mathbf{K}_{CE}$ (a 8 *x* 8 matrix in agreement with the FE adopted) is determined firstly by adding the flexibility matrix of the healthy shaft (without crack) to the additional flexibility matrix due to the crack (Cavalini Jr *et al*., 2016). In Eq. (1), $\mathbf{\Delta K = K - K}_{CE}$.

4. SHM TECHNIQUE

Figure 4 shows a flowchart to illustrate the crack identification methodology. The methodology begins with the application of the unbalance forces in the analyzed system, and the corresponding spectral responses are stored ($\mathbf{FFT}_{exp}$; Fast Fourier Transform). The same forces are applied to a representative FE model of the structure ($\mathbf{FFT}_{mod}$) so that the optimizer is responsible for adding the model of a crack with different depths and locations, randomly. The obtained spectral responses $\mathbf{FFT}_{mod}$ are compared with the experimental ones using two different objective functions DE_{OFA} and DE_{OFB} as shown by Eq. (7). If the procedure converges to a minimum value of the objective function tested, the crack is identified. If this is not the case, the optimization procedure will propose a new crack configuration (depth and location). The optimization process continues until convergence is achieved.

As mentioned, two configurations of the objective function are analyzed in this work aiming at improving the accuracy of the SHM technique to identify the crack location and depth, namely $DE_{OF\,A}$ and $DE_{OF\,B}$ as shows the Eq. (7). Note that the fitness evaluations associated with the sensors S_{8Z} and S_{28Z} are weighted by a factor 2 in $DE_{OF\,A}$. Differently, only the sensor S_{28Z} is weighted in $DE_{OF\,B}$.

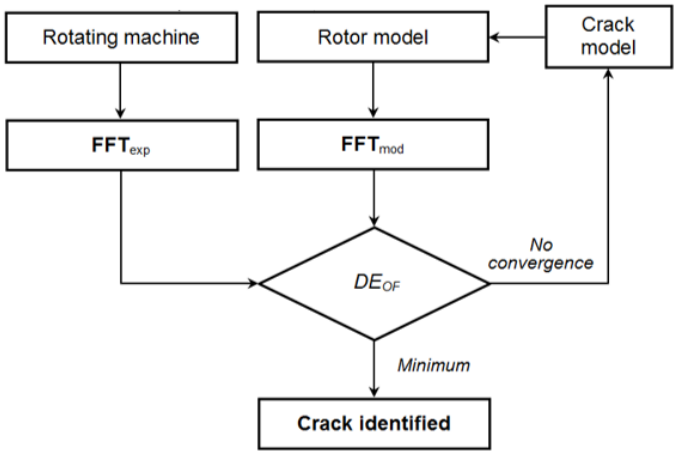

Figure 4. Crack identification flowchart.

$$DE_{OF\ A} = \frac{\left\|\mathbf{FFT}_{\exp,1} - \mathbf{FFT}_{\mathrm{mod},1}\right\|}{\left\|\mathbf{FFT}_{\exp,1}\right\|} + 2\frac{\left\|\mathbf{FFT}_{\exp,2} - \mathbf{FFT}_{\mathrm{mod},2}\right\|}{\left\|\mathbf{FFT}_{\exp,2}\right\|} + \frac{\left\|\mathbf{FFT}_{\exp,3} - \mathbf{FFT}_{\mathrm{mod},3}\right\|}{\left\|\mathbf{FFT}_{\exp,3}\right\|} + 2\frac{\left\|\mathbf{FFT}_{\exp,4} - \mathbf{FFT}_{\mathrm{mod},4}\right\|}{\left\|\mathbf{FFT}_{\exp,4}\right\|}$$

$$DE_{OF\ B} = \frac{\left\|\mathbf{FFT}_{\exp,1} - \mathbf{FFT}_{\mathrm{mod},1}\right\|}{\left\|\mathbf{FFT}_{\exp,1}\right\|} + \frac{\left\|\mathbf{FFT}_{\exp,2} - \mathbf{FFT}_{\mathrm{mod},2}\right\|}{\left\|\mathbf{FFT}_{\exp,2}\right\|} + \frac{\left\|\mathbf{FFT}_{\exp,3} - \mathbf{FFT}_{\mathrm{mod},3}\right\|}{\left\|\mathbf{FFT}_{\exp,3}\right\|} + 2\frac{\left\|\mathbf{FFT}_{\exp,4} - \mathbf{FFT}_{\mathrm{mod},4}\right\|}{\left\|\mathbf{FFT}_{\exp,4}\right\|} \tag{7}$$

The monitoring process was performed 10 times, considering 20 individuals in the initial population of the optimizer. Additionally, random noise was added to the dynamic responses of the rotating machine to simulate the experimental environment found in a real plant. Equation (8) indicates how noise was added to the responses.

$$\mathbf{q}_{noise} = \mathbf{q} + P_{noise}\mathbf{R}_{noise}\left\{E\left[\mathbf{q} - E(\mathbf{q})\right]^2\right\}^{1/2} \tag{8}$$

where $\mathbf{q}_{noise}$ is the noisy response, P_{noise} is the parameter that defines the amount of noise to be added (P_{noise} = 5%), and $\mathbf{R}_{noise}$ is the random noise. E [·] indicates the expected value of [·]. The vector $\mathbf{q}_{noise}$ is used to determine the $\mathbf{FFT}_{\exp}$ presented in Eq. (6) and Eq. (7).

In the present work, the heuristic optimization method DE was used to determine the crack configuration. DE was first proposed by Storn and Price (1995). DE represents a simple and efficient algorithm for finding global minima solutions. The DE algorithm is based on subsequently vector summing, which iteratively defines new searching directions (Lobato, 2008). Regarding the application of the considered SHM technique, the design space of the inverse problem is composed of two discrete variables: the *crack depth*, that can assume the values 0%, 5%, 10%, …, and 50% of the shaft diameter; and the *crack location*, which are the possible positions of the FE mesh that contain a cracked element. In this case, 25 finite elements were considered as potential candidate crack locations, which are: 5 to 11, 14 to 21, and 24 to 33 (see Fig. 1b).

As mentioned, displacement sensors are orthogonally mounted on the nodes #8 (S_{8X} and S_{8Z}) and #28 (S_{28X} and S_{28Z}) to collect the shaft vibration responses (see Fig. 1b). Thus, n = 4 in the objective function represented by Eq. (6). It is worth mentioning that the dynamic behavior of the rotating machine suffers the influence of the gravitational load along the vertical direction (i.e., Z direction). Therefore, it is expected that the nonlinear behavior induced by the crack on the system is more pronounced in the vibration responses collected by the sensors S_{8Z} and S_{28Z}.

5. NUMERICAL RESULTS

The crack identification results obtained by using the present SHM technique will be presented in this section, in which three rotation speeds are investigated: $\Omega = \Omega_{critical} / 2$ = 842.5 rev/min ($\Omega_{critical}$ = 1685 rev/min; first forward critical speed of the rotating machine), $\Omega = \Omega_{critical} / 3$ = 561.7 rev/min, and Ω = 1200 rev/min. The three different operating conditions are used to highlight the accuracy of the crack identification approach for a higher range of speeds. Additionally, for all results presented, an unbalance of $8x10^{-4}$ kgm/0º was considered only on disc D_1.

5.1 Operation Speed $\Omega = \Omega_{critical} / 3$

Breathing cracks induce 2X and 3X harmonic components on the vibration responses of the rotating machine (Bachschmid *et al.*, 2010). Therefore, it is expected that a strong 3X response may appear when the rotor is turning at one-third of its first critical speed. Figure 5 presents the vibration responses obtained by the sensor S_{28Z}, considering the shaft operating at $\Omega = \Omega_{critical} / 3 = 561.7$ rev/min.

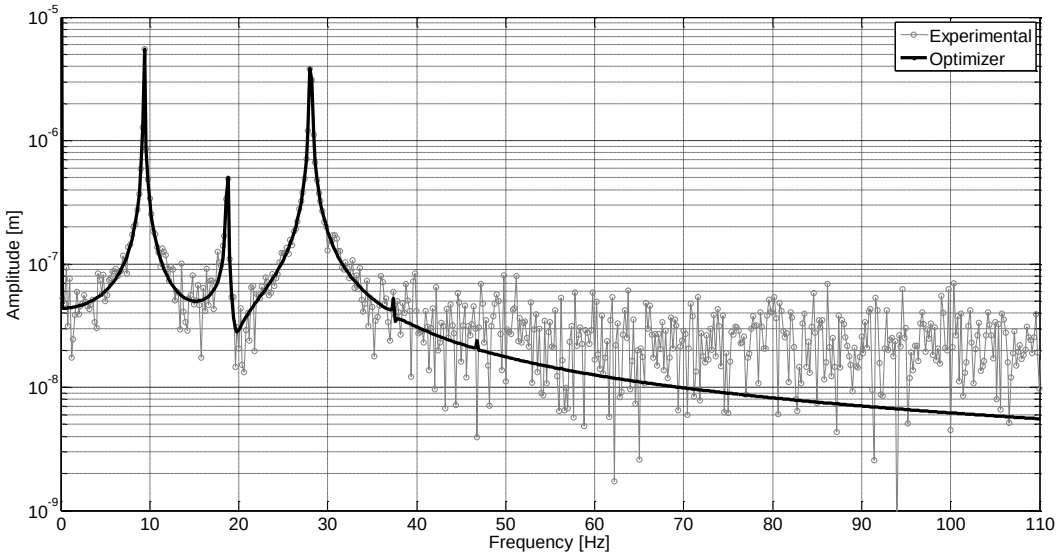

Figure 5. Vibration responses measured by the sensor S_{28Z} for the rotor operating at $\Omega = \Omega_{critical} / 3$ by using the objective function $DE_{OF\,A}$.

When using both the objective functions $DE_{OF\,A}$ and $DE_{OF\,B}$, the optimization process resulted in the successful estimations for the location and depth of the crack (10% crack depth). Figure 6 presents the vibration response obtained using the objective function $DE_{OF\,B}$. It is worth mentioning that only the fitness evaluations associated with the sensor S_{28Z} is weighted in $DE_{OF\,B}$.

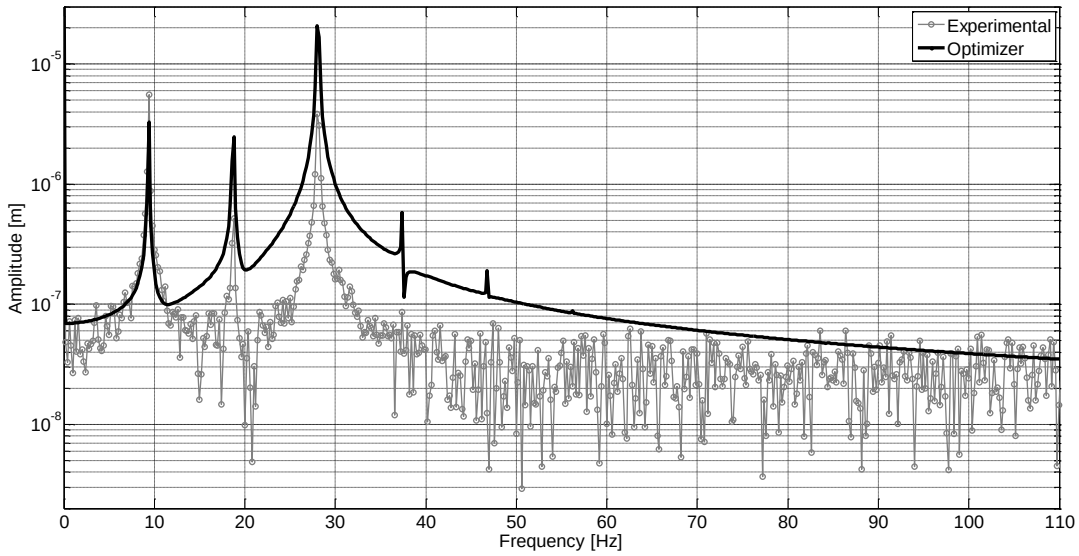

Figure 6. Vibration responses measured by the sensor S_{28Z} for the rotor operating at $\Omega = \Omega_{critical} / 3$ by using the objective function $DE_{OF\,B}$.

5.2 Operation Speed $\Omega = \Omega_{critical} / 2$

Figure 7 presents the vibration responses obtained using the sensor S_{28Z}, considering the shaft operating at $\Omega = \Omega_{critical} / 2 = 842.5$ rev/min, and the objective function $DE_{OF\,B}$. In this case, the crack was correctly identified (element #20 and 10% depth). However, for the objective function $DE_{OF\,A}$, the crack position could not be estimated correctly. In this case, a crack located at the element #21 with 10% depth was obtained (see Fig. 8).

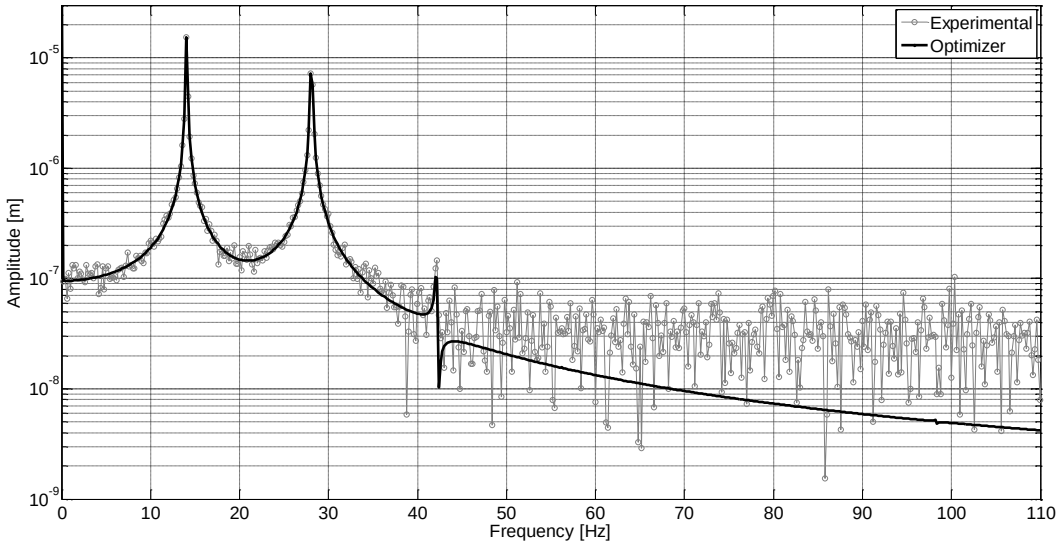

Figure 7. Vibration responses measured by the sensor S_{28Z} for the rotor operating at $\Omega = \Omega_{critical} / 2$ by using the objective function $DE_{OF\,B}$.

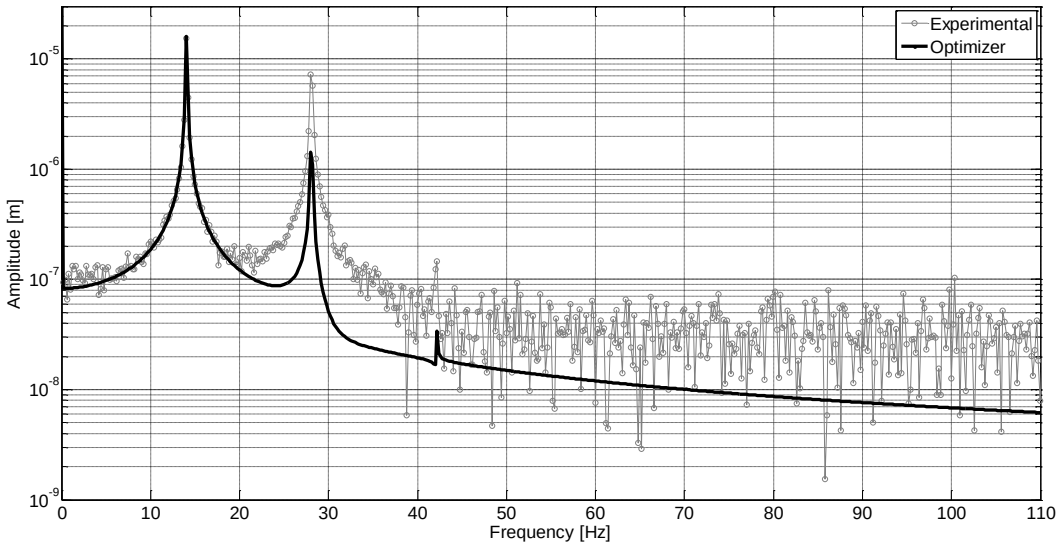

Figure 8. Vibration responses measured by the sensor S_{8Z} for the rotor operating at $\Omega = \Omega_{critical} / 2$ by using the objective function $DE_{OF\,B}$.

For this objective function ($DE_{OF\,A}$), the crack is correctly detected when it reaches 15% of depth. Thus, better results were obtained using the objective function $DE_{OF\,B}$.

5.3 Operation Speed Ω = 1200 rev/min

Since operating the rotor machine at the speeds $\Omega_{critical} / 2$ and $\Omega_{critical} / 3$ facilitates crack detection, other rotation speeds were tested. Figure 9 presents the vibration responses obtained by the sensor $S_{28Z,}$ considering the shaft operating at Ω = 1200 rev/min and a crack with 15% depth. Note that the 2X and 3X vibration components are small, which makes the crack identification harder. In this case, only cracks up to 15% depth were correctly identified by both objective functions.

Figure 10 presents the vibration responses for the same rotation speed for a crack with 10% depth. Note that the harmonic levels of vibration are small (below noise levels). For this reason, the optimizer could not correctly estimate the position and depth of the crack for Ω = 1200 rev/min. Even though the optimizer suggested a crack at element #21 with 10 % depth. This result can be associated with the variations in the 1X vibration amplitude due to the crack presence.

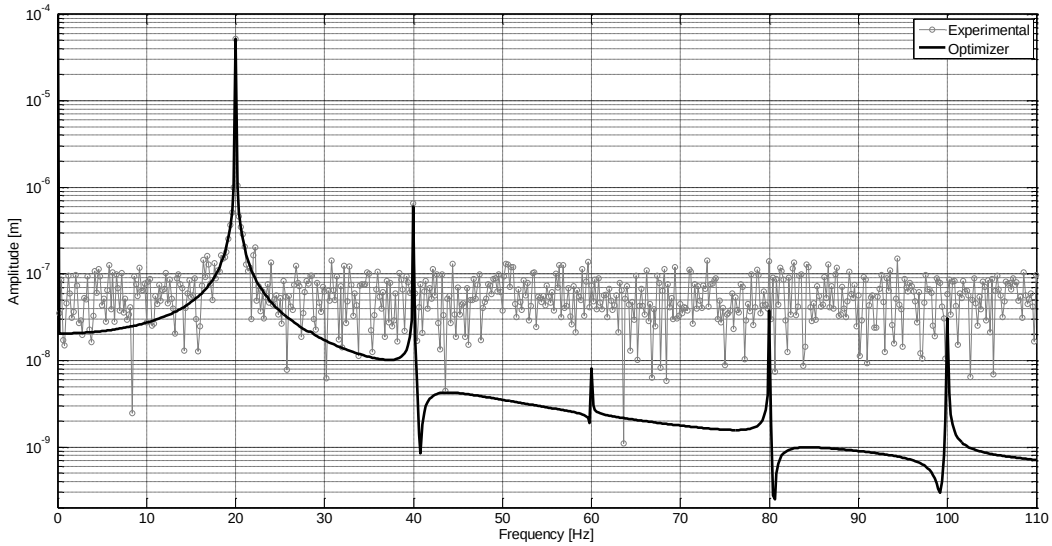

Figure 9. Vibration responses measured by the sensor S_{28Z} for the rotor operating at Ω = 1200 rev/min with a crack of 15% depth by using the objective function $DE_{OF\,B}$.

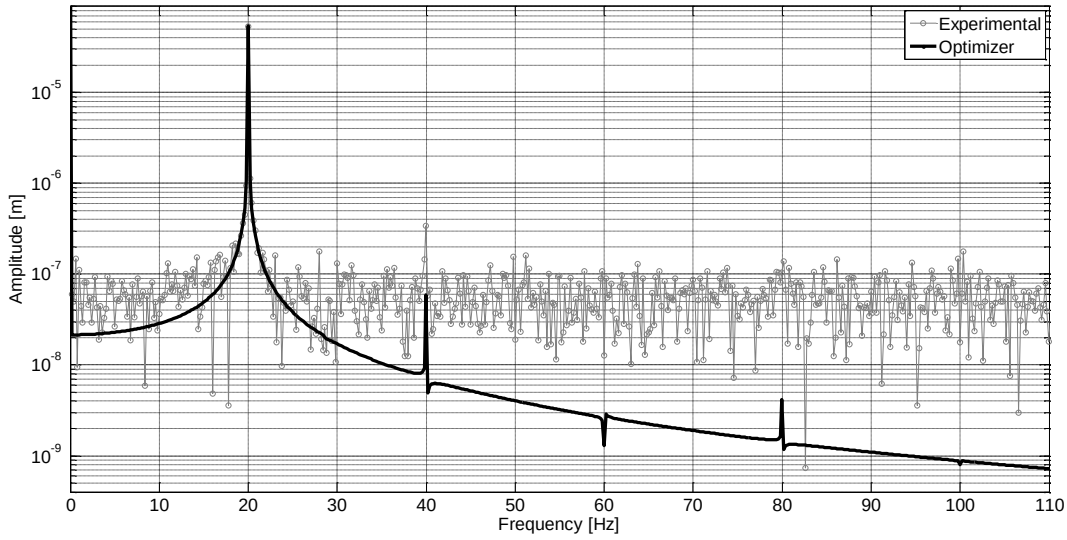

Figure 10. Vibration responses measured by the sensor S_{28Z} for the rotor operating at Ω = 1200 rev/min with a crack of 10% by using the objective function $DE_{OF\,B}$.

6. CONCLUSIONS

The obtained results demonstrate that the presented model-based approach can be helpful for fault identification, being able to determine the existence, location, and depth of transversal cracks along the shaft of a rotating machine. The evaluated SHM technique may be applied in industrial rotating machines if their representative models are available. One single sensor may be enough to obtain the correct crack identification. However, in different applications, more measurement points might be necessary to promote the correct damage identification. The presented SHM technique revealed to be efficient for different rotation speeds, especially for $\Omega = \Omega_{critical} / 2$ and $\Omega = \Omega_{critical} / 3$. Concerning the crack depth, this technique allowed the detection of transverse cracks from 15% depth. Two different objective functions were compared, namely $DE_{OF\,A}$ and $DE_{OF\,B}$. The obtained results indicated that the accuracy of the identification is higher when only the sensor located close to the position of the crack was considered. Further studies will encompass an experimental validation of the proposed SHM technique.

7. ACKNOWLEDGMENTS

The authors are thankful for the financial support provided to the present research effort by CNPq (574001/2008-5, 304546/2018-8, and 431337/2018-7), FAPEMIG (TEC-APQ-3076-09, TEC-APQ-02284-15, TEC-APQ-00464-16, and PPM-00187-18), and CAPES through the INCT-EIE.

8. REFERENCES

Bachschmid, N., Pennacchi, P., & Tanzi, E., 2000. "Identification of Transverse Crack Position and Depth in Rotor Systems". *Meccanica*, Vol. 35, No. 6, pp. 563-582.

Burbano, C. R., & Steffen Jr., V., 2007. "Diagnosis of cracked shafts by monitoring the transient motion response". *International Symposium on Dynamic Problems of Mechanics - XII Diname, 2007, Ilhabela - SP., Proc. of IMAC-XXV: Conference & Exposition on Structural Dynamics*, pp. 1-10.

Carden, E. P., & Fanning, P., 2004. "Vibration based condition monitoring: a review". *Structural Health Monitoring*, Vol. 3, No. 5, pp. 355-377.

Cavalini Jr., A. A., Lara-Molina, F. A., Sales, T. P., & Steffen Jr., V., 2015. "Uncertainty Analysis of a Flexible Rotor Supported by Fluid Film Bearings". *Latin American Journal of Solids and Structures*, Vol.12, pp. 1487-1504.

Cavalini Jr., A. A., Sanches, L., Bachschmid, N., & Steffen Jr., V. , 2016. "Crack identification for rotating machines based on a nonlinear approach". *Mechanical Systems and Signal Processing* Vol.1, pp. 1-14.

Dimarogonas, A. D., Paipetis, S. A., & Chondros, T. G. , 2013. *Analytical Methods in Rotor Dynamics.* Springer Netherlands, 2nd edition.

Doebling, S. W., Farrar, C. R., & Prime, M. B. , 1998. "A summary review of vibration-based damage identification methods". *Shock and Vibration Digest* Vol. 30, pp. 91-105.

Gasch, R. , 1976. "Dynamic behaviour of a simple rotor with a cross-sectional crack". *Proceedings of the International Conference on Vibrations in Rotating Machinery, Institute of Mechanical Engineers*. New York, pp. 123-128.

Isermann, R. , 1995. "Model Based Fault Detection and Diagnosis Methods". *Proceeding of the American Control Conference*, Vol. 3, pp. 1605-1609.

Lalanne, M., & Ferraris, G. , 1998. *Rotordynamics Prediction in Engineering.* Baffins Lane, Chichester: John Wiley and Sons Ltd.

Lobato, F. S. , 2008. *Otimização Multi-Objetivo para o Projeto de Sistemas de Engenharia.* Tese de Doutorado apresentada ao programa de Pós-Graduação em Eng. Mecânica, da Universidade Federal de Uberlândia.

Markert, R., Platz, R., & Seidler, M. , 2001. "Model Based Fault Identification in Rotor Systems by Least Squares Fitting". *International Journal of Rotating Machinery*, Vol. 7, No. 5, pp. 311-321.

Mayes, I. W., & Davis, W. R. , 1976. "The Vibrational Behaviour of a Cracked Shaft Containing a Transverse Crack". *IME Conf. Vibrations in Rotating Machinery* Vol. 168, No. 6.

Morais, T. S., Der Hagopian, J., Steffen Jr., V., & Mahfoud, J. , 2014. "Optimization of unbalance distribution in rotating machinery whith localized non linearity". *Mechanism and Machine Theory* Vol 72, pp. 60-70.

Saavedra, P. N., & Cuitiño, L. A. , 2001. "Crack Detection and Vibration Behavior of Cracked Beams". *Computers & Structures* Vol. 79, No. 16, pp. 1451-1459.

Sawicki, J. T., Friswell, M. I., Kulesza, Z., Wroblewski, A., & Lekki, J. D. , 2011. "Detecting Cracked Rotors Using Auxiliary Harmonic Excitation". *Journal of Sound and Vibration*, Vol. 330, pp. 1365-1381.

Storn, R., & Price, K. , 1995. "Differential Evolution: A Simple and Efficient Adaptative Scheme for Global Optimization over Continuous Spaces". *International Computer Science Institute*, Vol. 12, No. 1, pp. 1-16.

Zhao, J. , 2013. *Vibration Based Damage Identification of Time-Varying Dynamical Systems.* PhD Thesis, University of Tennessee.

9. RESPONSIBILITY NOTICE

The authors are the only responsible for the printed material included in this paper.